Breakdown in Repression of IFN-γ mRNA Leads to Accumulation of Self-Reactive Effector CD8$^+$ T Cells

Pheh-Ping Chang,* Sau K. Lee,* Xin Hu,* Gayle Davey,† Guowen Duan,* Jae-Ho Cho,‡ Guna Karupiah,§ Jonathan Sprent,‡ William R. Heath,† Edward M. Bertram,§ and Carola G. Vinuesa*

Tight regulation of virus-induced cytotoxic effector CD8$^+$ T cells is essential to prevent immunopathology. Naturally occurring effector CD8$^+$ T cells, with a KLRG1^{hi} CD62L^{lo} phenotype typical of short-lived effector CD8$^+$ T cells (SLECs), can be found in increased numbers in autoimmune-prone mice, most notably in mice homozygous for the *san* allele of *Roquin*. These SLEC-like cells were able to trigger autoimmune diabetes in a susceptible background. When Roquin is mutated (*Roquin^{san}*), effector CD8$^+$ T cells accumulate in a cell-autonomous manner, most prominently as SLEC-like effectors. Excessive IFN-γ promotes the accumulation of SLEC-like cells, increases their T-bet expression, and enhances their granzyme B production in vivo. We show that overexpression of IFN-γ was caused by failed posttranscriptional repression of *Ifng* mRNA. This study identifies a novel mechanism that prevents accumulation of self-reactive cytotoxic effectors, highlighting the importance of regulating *Ifng* mRNA stability to maintain CD8$^+$ T cell homeostasis and prevent CD8-mediated autoimmunity. *The Journal of Immunology*, 2012, 189: 701–710.

Cytotoxic CD8$^+$ effector T cells are an important component of the adaptive immune response against intracellular pathogens, including viruses, some bacteria, and tumor cells. As is true for other arms of the immune response, the trade off for being able to mount potent cytotoxic responses against pathogen-infected cells is the risk for autoimmunity. Breakdown in CD8$^+$ T cell tolerance plays a major role in the development of type 1 diabetes and contributes to multiple sclerosis (1–4). Expansion of autoreactive CD8$^+$ effector T cells has also been associated with other autoimmune diseases, including pancreatitis, autoimmune gastritis, inflammatory bowel disease, and systemic lupus erythematosus (5–8). Over the past few decades, we have gained considerable understanding about the cellular and molecular mechanisms that drive CD8$^+$ effector T cell differentiation and clonal expansion during infection. There is relatively less known about the mechanisms that prevent expansion of self-reactive CD8$^+$ T cells and/or their maturation into terminally differentiated effector cells.

CD8$^+$ T cells responding to viral infections initiate their maturation into effector cells by upregulating the transcription factors T-bet and Eomesodermin (9–11). Terminal differentiation into CD8$^+$ short-lived effector cells (SLECs) requires further upregulation of T-bet and high expression of Blimp-1 (12-14). The metabolic regulator mTOR plays a crucial role in CD8$^+$ T cell development through its ability to sustain T-bet expression (15). In addition to this important cell-autonomous transcriptional control of CD8$^+$ T cell differentiation, extrinsic influences exerted by cytokines play a critical role in regulating CD8$^+$ effector expansion, as well as survival. IL-15, either alone or together with IL-7, can promote the survival of SLECs and KLRG1^{lo}CD127^{hi} effector cells (12, 16), respectively, during viral infections. IFN-γ was shown to support the expansion of CD8$^+$ effectors (17).

Contraction of effector cells is essential to maintain CD8$^+$ T cell homeostasis and prevent accumulation of potentially self- or cross-reactive cells and immunopathology. This is particularly important because thymic clonal deletion ensures elimination of high-avidity self-reactive T cells but allows low- and intermediate-avidity self-reactive T cells to escape to the periphery (18). These can cause immunopathology if they are recruited into antiviral responses and fail to contract postinfection. In addition to T cell anergy, activation-induced cell death and the proapoptotic molecule Bim keep autoreactive CD8$^+$ T cells in check (19–21). Extrinsic mechanisms also operate to repress self-reactive T cells; these include availability of cytokines, such as IL-7 and IL-15 (22, 23), and the suppressive effect of regulatory T cells through their ability to secrete IL-10 and TGF-β (24). Although IFN-γ was shown to promote CD8$^+$ T cell apoptosis during viral infection (25), a role for IFN-γ in the regulation of self-reactive CD8$^+$ T cell effectors has not been described.

In the absence of immunization, activated effector CD8$^+$ T cells are found in mice bred in specific pathogen-free conditions, some of which express high amounts of the SLEC marker, KLRG1 (26).

*Department of Pathogens and Immunity, John Curtin School of Medical Research, Australian National University, Canberra 2601, Australian Capital Territory, Australia; †Department of Microbiology and Immunology, The University of Melbourne, Parkville 3010, Victoria, Australia; ‡Immunology Research Program, Garvan Institute of Medical Research, Darlinghurst 2010, New South Wales, Australia; and §Department of Immunology, John Curtin School of Medical Research, Australian National University, Canberra 2601, Australian Capital Territory, Australia

Received for publication August 24, 2011. Accepted for publication May 7, 2012.

This work was supported by a Viertel Senior Medical Research Fellowship (to C.G.V.), National Health and Medical Research Council program grants (to C.G.V., J.S., and W.R.H.), and National Institutes of Health Contract BAA-NIAID-DAIT-07-35 (to E.M.B. and G.K.).

All datasets have been submitted to the National Center for Biotechnology Information/Gene Expression Omnibus (http://www.ncbi.nlm.nih.gov/geo/) under accession number GSE37319.

Address correspondence and reprint requests to Prof. Carola G. Vinuesa, Department of Pathogens and Immunity, John Curtin School of Medical Research, Australian National University, Canberra, ACT 2601, Australia. E-mail address: carola.vinuesa@anu.edu.au

This online version of this article contains supplemental material.

Abbreviations used in this article: JCSMR, John Curtin School of Medical Research; MFI, mean fluorescence intensity; mOVA, membrane-bound OVA; RIP, rat insulin promoter; SLEC, short-lived effector cell; Tfh, follicular helper T.

In a separate study, an effector CD122^{lo} and MHC class I-dependent CD8$^+$ population was also described in unimmunized mice (27). It is unclear whether KLRG1^{hi} effector CD8$^+$ T cells found in unimmunized mice can mediate autoimmune disease.

Roquin is a RING-1/CCCH-type zinc finger protein that controls the expression of ICOS (*Icos*) mRNA posttranscriptionally. Loss of Roquin, either specifically on T cells or in the hematopoietic system, caused expansion on CD8$^+$ effector-like T cells but not autoimmunity (28). In contrast, Roquin bearing the *san* allele, which is a gain-of-function-allele (29, data not shown), causes follicular helper T (Tfh) cell-dependent lupus (30–33); it is achieved, at least in part, through posttranscriptional regulation of *Icos* mRNA. In this article, we show that *sanroque* mutation of Roquin causes the accumulation of naturally occurring KLRG1^{hi} CD8$^+$ effector cells, which can trigger autoimmune diabetes. The *sanroque* mutation causes failure of the posttranscriptional control of *Ifng* mRNA that leads to excessive IFN-γ signaling, and this is a major driver of SLEC-like cell accumulation with enhanced effector features.

Materials and Methods

Mice

The mice were housed in specific pathogen-free conditions at the Australian National University Bioscience Facility. *Roquin$^{san/san}$* C57BL/6 mice were crossed to *Tbx21$^{Dii/Dii}$*, OT-I, and *Ifngr1$^{-/-}$* mice; *Aire$^{-/-}$*, *Cblb$^{-/-}$*, B6.*Yaa*, and *Fas$^{The/The}$* mice are all on a C57BL/6 background. *Fas$^{The/The}$* mice carry a loss-of-function point mutation at the *Fas* gene that results in high titers of antinuclear Ab (ANA$^+$) in the mice, as well as an accumulation of double-negative T cells in the periphery as the mice age; in these respects, they are very similar to the *Fas$^{lpr/lpr}$* mice strain (L. Tze and C. Goodnow, unpublished observations). RIP-mOVA mice, which express membrane-bound OVA (mOVA) in their pancreatic β cells under the control of rat insulin promoter (RIP), were bred at the University of Melbourne, transferred to the Australian Bioscience Services for experiments, and allowed to acclimatize at this facility for 1 wk prior to injection. All animal procedures were approved by the Australian National University Animal Ethics and Experimentation Committee.

Bone marrow chimeras

Recipient mice were sublethally irradiated with 900 cGy (450 cGy in two doses) and were reconstituted via i.v. injection with 2×10^6 donor bone marrow cells.

OT-I cell preparation for adoptive transfer

OT-I T cells were purified from the spleens and pooled lymph nodes of OT-I mice (*Roquin$^{san/san}$* or *Roquin$^{+/+}$* mice) using the CD8a$^+$ T cell Isolation kit II (MACS; Miltenyi Biotec). To transfer CD44^{lo} OT-I T cells, OT-I T cells were sorted from the spleens and pooled lymph nodes using a FACSAria (BD Biosciences).

Adoptive-transfer experiments

Purified OT-I cells were spiked with fixed numbers of B cells prior to i.v. injection into nonirradiated RIP-mOVA recipients. The urine of recipient mice was collected to assess glucosuria by Uristix (Bayer). Mice with glucose concentrations ≥55 mmol/l were considered diabetic.

Abs

All FACS Abs used were from BD Pharmingen, with the exception of anti-mouse CD8a–PE–Cy7 (53-6.7; BioLegend), anti-mouse KLRG1-allophycocyanin (2F1; eBioscience), anti-mouse KLRG1–PE–Cy7 (2F1; eBioscience), anti-mouse CD127 (IL-7Rα)-PE (A7R34; BioLegend), anti-mouse CD62L (L-selectin)–PerCP–Cy5.5 (MEL-14; eBioscience), anti-mouse/human CD44-Pacific Blue (IM7; BioLegend), anti-human/mouse T-bet–PerCP.Cy5.5 (4B10; eBioscience), and mouse anti-human granzyme B-PE (GB11; Invitrogen).

Flow cytometry

Spleen and lymph node cell suspensions were prepared by sieving and gentle pipetting. For surface staining, cells were maintained in the dark at 4°C throughout. Cells were incubated in FACS buffer with each Ab for 20 min and washed thoroughly with FACS buffer. For intracellular staining, cells were fixed and permeabilized using the Mouse Regulatory T Cell Staining Kit (eBiosciences), following the manufacturer's instructions. Flow cytometers (FACSCalibur and LSR II; BD) and software (CellQuest or FACSDiva, respectively; BD) were used for the acquisition of flow cytometric data, and FlowJo software (Tree Star) was used for analysis.

In vitro stimulation

Splenocytes from unimmunized mice were stimulated with 500 ng/ml ionomycin, 50 ng/ml PMA, and 1:250 GolgiStop for 4 h at 37°C before being subjected to IFN-γ staining.

Histology

Pancreases were fixed in 10% neutral-buffered formalin, embedded in paraffin wax, sectioned at 4 μm thickness, dewaxed, and stained with H&E.

Gene-expression profiling

For gene-expression analysis, *Roquin$^{san/san}$* and *Roquin$^{+/+}$* CD44^{lo} CD8$^+$ T cells were sorted, and RNA was isolated using TRIzol reagent (Invitrogen), followed by a second isolation using RNeasy (QIAGEN). RNA was amplified twice and hybridized to GeneChip Mouse Gene 1.0 ST Array (Affymetrix) by the Australian Cancer Research Foundation Biomolecular Resource Facility (John Curtin School of Medical Research [JCSMR]). Data were analyzed using Partek software. The *t* test was used to identify significantly differently expressed genes ($p \leq 0.05$) between *Roquin$^{san/san}$* and *Roquin$^{+/+}$* CD44^{lo} CD8$^+$ T cells samples ($n = 3$/group).

All datasets have been deposited at National Center for Biotechnology Information/Gene Expression Omnibus under accession number GSE37319 (http://www.ncbi.nlm.nih.gov/geo/query/acc.cgi?acc=GSE37319).

In vitro cell activation

A total of 5×10^5 sorted CD44^{lo} CD8$^+$ T cells was activated in the presence of 5 μg/ml anti-CD3 (BD Pharmingen), 2 μg/ml anti-CD28 (BD Pharmingen), and 10 ng/ml recombinant mouse IL-12p70 (eBioscience) for 16 h.

Actinomycin D treatment

The transcriptional inhibition reagent actinomycin D (10 μg/ml) was added to the media for resuspension of in vitro-activated CD8$^+$ T cells. Cells in triplicate wells were harvested at 0, 0.5, 1, or 3 h. Cells were then subjected to RNA extraction with TRIzol reagent, followed by *Ifng* real-time PCR.

Real-time PCR

RNA was isolated with TRIzol reagent (Invitrogen). cDNA was synthesized using M-MLV Reverse Transcriptase (Invitrogen). Inventoried TaqMan Gene Expression Assays (Applied Biosystems) were used to amplify *Tbx21* (Mm00450960_m1) and *Gapdh* (Mm99999915_g1) sequences. *Ifng*, *Roquin*, *Hprt*, and *β-actin* cDNA were amplified using Power SYBR Green PCR Master Mix (Applied Biosystems). Primers for *Ifng* were: 5′-ACAGCAAGGCGAAAAAGGAT-3′ and 5′-TGAGCTCATTGAATGCTTGG-3′; primers for *Roquin* were: 5′-CGTATTGATTGTATGTGATTGTG-3′ and 5′-AGCCATCTCTATTCTGACTC-3′; primers for *β-actin* were: 5′-TATGGAATCCTGTGGCATC-3′ and 5′-GTGTTGGCATAGAGGTCTT-3′; and primers for *Hprt* were: 5′-AGCAGTACAGCCCCAAAATG-3′ and 5′-AGAGGTCCTTTTCACCAGCA-3′. Real-time PCR was quantified with an ABI 7900 Prism, and fold changes in expression were determined by the $2^{-\Delta\Delta Ct}$ method, with the results normalized to *Hprt* for *Ifng*, *β-actin* for *Roquin*, or *Gapdh* for *Tbx21*.

Statistical analyses

Data were analyzed using the Mann–Whitney *U* test, with the exception of bone marrow chimera and *Ifng* mRNA-expression experiments, for which the paired *t* test and unpaired *t* test was used, respectively. Unless otherwise stated, each symbol represents one mouse, and bars represent the median values for each group.

Results

SLEC-like CD8$^+$ T cells are increased in mice prone to autoimmune disease

Terminally differentiated cytotoxic KLRG1^{hi} CD127^{lo} SLEC CD8$^+$ T cells reacting to viral Ags are induced upon primary response to virus infection (12). The existence of small numbers of

KRLG1^{hi} CD8^{+} T cells, possibly reacting to self-Ag, in unimmunized healthy C57BL/6 mice (26, 27), led us to hypothesize that their numbers would be higher in mouse strains prone to autoimmune disease. Given that these KRLG1^{hi} CD8^{+} T cells resembled virus-induced SLECs—they expressed low levels of CD62L, CD127, and CD122; at least 40% were in cell cycle (Ki-67^{+}); and, unlike naive cells, died rapidly ex vivo in a manner comparable to virus-induced SLECs (Fig. 1A–C)—we refer to these cells hereafter as "SLEC-like" cells. We investigated SLEC-like cell numbers in five strains of mice on a C57BL/6 background that develop severe (*Roquin*$^{san/san}$) or mild (*Aire*$^{-/-}$, *Cbl-b*$^{-/-}$, *Fas*$^{The/The}$) autoimmunity or fail to develop autoimmunity (B6.*Yaa*). Statistically significant increases in SLEC-like cells were found in the four strains that develop overt autoimmune symptoms (Fig. 1D) but not in B6.*Yaa* mice; the *Yaa* gene by itself is unable to induce significant autoimmune responses in mice without the BXSB/MpJ background (34). Among the mice prone to autoimmune disease, *Roquin*$^{san/san}$ mice, which were previously shown to develop lupus and be more susceptible to autoimmune diabetes (32), had by far the highest proportion of SLEC-like CD8^{+} T cells, with an increase detected as early as 7 wk of age (Fig. 1D). Hence, we decided to use *Roquin*$^{san/san}$ mice to investigate the regulation of SLEC-like cells.

Given the recently reported CD8^{+} effector-like T cell expansion in Roquin-deficient mice (28), we assessed *Roquin* mRNA expression in *Roquin*$^{san/san}$ CD8^{+} T cells. Sorted CD44^{lo} CD8^{+} T cells were activated in the presence of anti-CD3, anti-CD28, and IL-12 for 16 h. Real-time PCR revealed an ~4-fold reduction in the *Roquin* mRNA level in both *Roquin*$^{+/+}$ and *Roquin*$^{san/san}$ activated CD8^{+} T cells compared with naive CD8^{+} T cells. Roquin

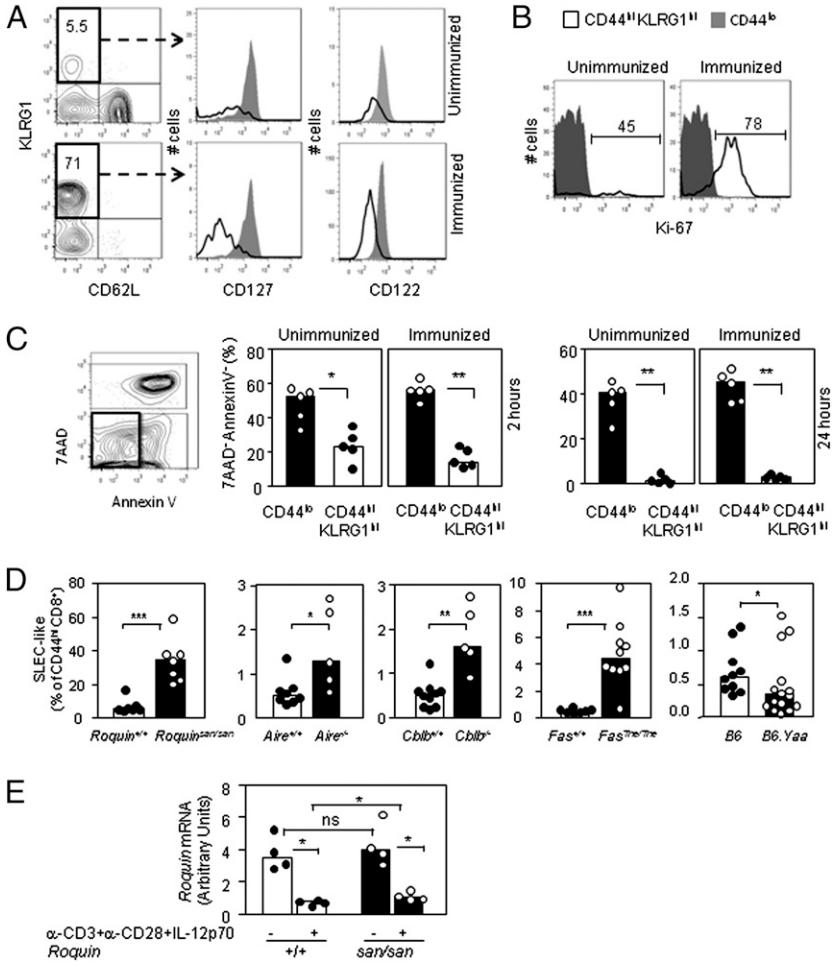

FIGURE 1. KLRG1^{hi} CD8^{+} T cells resemble virus-reactive SLECs and are increased in mice prone to autoimmune disease. (**A**) Representative flow cytometric contour plots showing KLRG1^{hi}CD62L^{lo} cells among CD8^{+} CD44^{hi} spleen cells from unimmunized C57BL/6 mice (*top left panel*) and D^{b}/NP366-374–specific KLRG1^{hi}CD62L^{lo} cells from C57BL/6 mice 8 d after a secondary challenge with influenza A/PR8/34 virus, which are serologically distinct from A/HKx31 (*bottom left panel*). Flow cytometric graphs show CD127 (IL-7Rα) (*middle panels*) and CD122 (IL-2/IL-15Rβ) (*right panels*) fluorescence intensity in KLRG1^{lo}CD62L^{hi} (filled histograms) and KLRG1^{hi}CD62L^{lo} (open histograms) CD8^{+} CD44^{hi} spleen cells from unimmunized and immunized C57BL/6 mice. Numbers represent the percentage of cells in the indicated gates. (**B**) Proportion of proliferating Ki-67^{+} cells among CD44^{hi} KLRG1^{hi} CD8^{+} and naive CD44^{lo} T cells from unimmunized mice (*left panel*) and mice 7 d postprimary challenge with influenza virus (*right panel*). Numbers represent the percentage of cells in the indicated gates. (**C**) Representative contour plot showing the gating strategy to identify live (7AAD^{-} Annexin V^{-}) CD8^{+} T cells (*left panel*). Bar graphs show live cells among naive (CD44^{lo} CD8^{+}) and CD44^{hi}KLRG1^{hi} CD8^{+} T cells from splenic cells incubated at 37°C in culture media for 2 or 24 h after harvesting. (**D**) Bar graphs showing the proportion of SLEC-like cells (KLRG1^{hi}CD62L^{lo}) among CD44^{hi} CD8^{+} T cells in the blood of mice. (**E**) Bar graph showing *Roquin* mRNA normalized to *β-actin* in sorted CD44^{lo} CD8^{+} T cells of *Roquin*$^{+/+}$ (open bars) and *Roquin*$^{san/san}$ (black bars) mice in the absence or the presence of α-CD3, α-CD28, and IL-12p70 after 16 h of in vitro culture. Each symbol represents one mouse (C, D) or the average values of technical triplicates of one mouse (E). In (C)–(E), bars represent the median values for each group. All data are representative of two independent experiments. *$p < 0.05$, **$p < 0.005$, ***$p < 0.0005$.

expression was comparable between *Roquin*$^{+/+}$ and *Roquin*$^{san/san}$ naive CD8$^+$ T cells. Activated *Roquin*$^{san/san}$ CD8$^+$ T cells expressed slightly more *Roquin* (Fig. 1E). Together, this indicates that the accumulation of SLEC-like CD8$^+$ T cells in *Roquin*$^{san/san}$ mice cannot be attributed to reduced *Roquin* expression.

Roquin^{san} *acts cell autonomously to promote accumulation of SLEC-like cells*

Autoimmune-prone *Roquin*$^{san/san}$ mice have an accumulation of CD4$^+$ and CD8$^+$ activated/memory T cells (32). In-depth analysis revealed an ~3-fold increase in *Roquin*$^{san/san}$ CD8$^+$ T cells in 7–8-wk-old *Roquin*$^{san/san}$ mice compared with *Roquin*$^{+/+}$ littermates (Fig. 2A). The increase in total CD8$^+$ T cells was due to accumulation of effector and/or memory CD44^{hi} CD8$^+$ T cells (Fig. 2A). To determine which CD44^{hi} CD8$^+$ subsets were dysregulated in *Roquin*$^{san/san}$ mice, expression of CD62L and KLRG1 was assessed. Effector T cells downregulate CD62L to circulate to inflamed tissues, whereas resting memory T cells maintain its expression; KLRG1 is a marker of terminally differentiated SLECs. The most prominent expansion of *Roquin*$^{san/san}$ effectors occurred among KLRG1^{hi} CD62L^{lo} SLEC-like cells, whose frequency was increased by 19-fold. There was a less-pronounced (2-fold) increase in the frequency of non–SLEC-like (KLRG1^{lo} CD62L^{lo}) effectors in *Roquin*$^{san/san}$ mice (Fig. 2B). *Roquin*^{san} did not significantly increase the absolute numbers of resting memory phenotype (KLRG1^{lo} CD62L^{hi}) CD8$^+$ T cells (Fig. 2B, *bottom panel*).

To investigate whether *Roquin*^{san} acts cell autonomously to induce the accumulation of SLEC-like cells, as well as whether non-hematopoietic cells contribute to this effect, two sets of mixed bone marrow chimeras were constructed. In the first set, *Roquin*$^{san/san}$

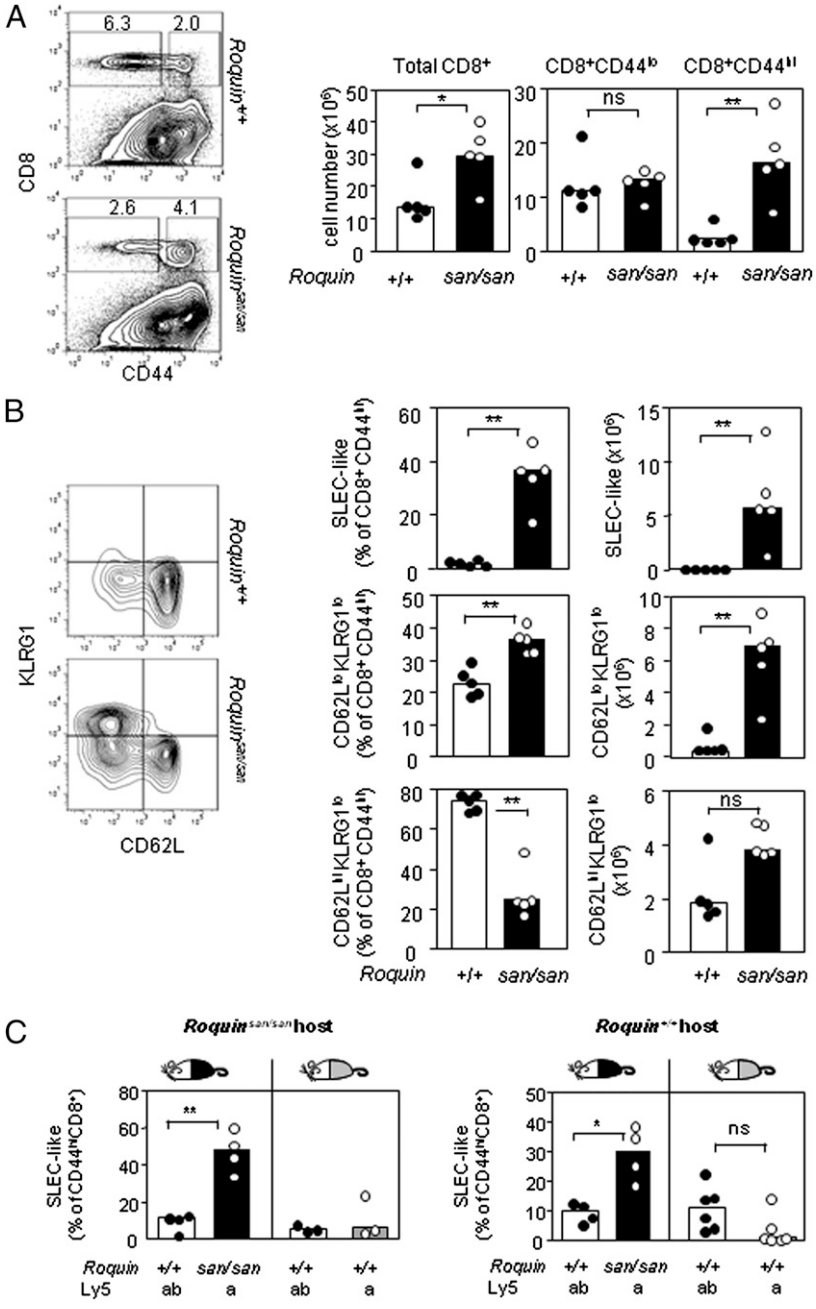

FIGURE 2. Accumulation of KLRG1^{lo} effector and SLEC-like CD8$^+$ T cells in *Roquin*$^{san/san}$ mice. (**A**) Representative flow cytometric contour plots showing CD44^{lo} and CD44^{hi} cells among CD8$^+$ spleen cells in 7–8-wk-old unimmunized *Roquin*$^{+/+}$ (*top left panel*) and *Roquin*$^{san/san}$ (*bottom left panel*) mice. Numbers represent the percentage of cells in the indicated gates. *Right panels*, Bar graphs enumerating total CD8$^+$, CD44^{lo}CD8$^+$, and CD44^{hi}CD8$^+$ T cells from 7–8-wk-old unimmunized *Roquin*$^{+/+}$ (open bars) and *Roquin*$^{san/san}$ (black bars) mice. (**B**) Representative flow cytometric contour plots showing CD62L^{lo} KLRG1^{hi} (SLEC-like), CD62L^{lo}KLRG1^{lo} (non–SLEC-like effector), and CD62L^{hi}KLRG1^{lo} (resting memory phenotype) cells among CD8$^+$CD44^{hi} spleen cells from *Roquin*$^{+/+}$ (*top left panel*) and *Roquin*$^{san/san}$ (*bottom left panel*) mice. Bar graphs (*right panels*) showing percentage (*left column*) and numbers (*right column*) of SLEC-like cells (*top panels*), CD62L^{lo} KLRG1^{lo} (*middle panels*), and CD62L^{hi} KLRG1^{lo} (*bottom panels*) cells among CD44^{hi} CD8$^+$ spleen cells from *Roquin*$^{+/+}$ (open bars) and *Roquin*$^{san/san}$ (filled bars) mice. (**C**) Percentages of Ly5ab and Ly5a of SLEC-like cells of 9-wk 1:1 mixed bone marrow chimeras reconstituted with either *Roquin*$^{+/+}$ Ly5ab and *Roquin*$^{san/san}$ (*sanroque*) Ly5a bone marrow (*left panels* within bar graphs) or *Roquin*$^{+/+}$ Ly5ab and *Roquin*$^{+/+}$ Ly5a bone marrow (*right panels* within bar graphs); bone marrow recipients are sublethally irradiated *Roquin*$^{san/san}$ Ly5b mice (*left panel*) or *Roquin*$^{+/+}$ Ly5b mice (*right panel*). Statistical analysis comparing CD8$^+$ T cell subsets from the same chimeric mice was performed using the paired *t* test. Each symbol represents one mouse, and bars represent the median values for each group. Data are representative of five (A, B) experiments, three independent experiments (C, *right panel*), or one experiment (C, *left panel*). $*p < 0.05$, $**p < 0.005$.

Ly5b mice were sublethally irradiated and reconstituted with either a 1:1 mix of *Roquin*$^{+/+}$ Ly5ab and *Roquin*$^{san/san}$ Ly5a bone marrow or a 1:1 mix of *Roquin*$^{+/+}$ Ly5ab and *Roquin*$^{+/+}$ Ly5a bone marrow. In a second set of chimeras, recipient *Roquin*$^{+/+}$ Ly5b mice were sublethally irradiated and reconstituted with either a 1:1 mix of *Roquin*$^{+/+}$ Ly5ab and *Roquin*$^{san/san}$ Ly5a bone marrow or a 1:1 mix of *Roquin*$^{+/+}$ Ly5ab and *Roquin*$^{+/+}$ Ly5a bone marrow. SLEC-like CD8$^+$ T cells derived from *Roquin*$^{san/san}$ Ly5a progenitors were increased by 5- and 3-fold compared with those derived from *Roquin*$^{+/+}$ Ly5ab in *Roquin*$^{san/san}$ hosts and *Roquin*$^{+/+}$ hosts, respectively (Fig. 2C). Together, these indicate that the accumulation of *Roquin*$^{san/san}$ SLEC-like cells is CD8$^+$ T cell intrinsic, and the nonhematopoietic system in *Roquin*$^{san/san}$ mice may enhance this effect.

Expansion of SLEC-like cells is associated with autoimmune diabetes

To investigate whether abnormal SLEC-like CD8$^+$ T cell expansion in *Roquin*$^{san/san}$ mice may contribute to autoimmune diabetes, we investigated SLEC-like cell accumulation and diabetes induction after adoptive transfer of *Roquin*$^{san/san}$ OT-I cells into RIP-mOVA mice (35). In our study, injection $>5 \times 10^6$ OT-I cells into nonirradiated RIP-mOVA recipients led to diabetes induction, whereas 2×10^6 OT-I cells rarely caused disease (data not shown). This is somewhat less efficient than originally reported (35). To examine the effect of the *san* mutation at conditions unlikely to cause diabetes with wild-type cells, we injected 1×10^6 OT-I cells from either *Roquin*$^{san/san}$ or *Roquin*$^{+/+}$ mice into nonirradiated RIP-mOVA recipients. The adoptively transferred OT-I cells were spiked with a fixed number of B cells to control for variations in the inoculum.

The phenotype of OT-I donor cells from young *Roquin*$^{san/san}$ and *Roquin*$^{+/+}$ mice was investigated prior to transfer: only 0.5% KLRG1^{hi} cells were present in the *Roquin*$^{san/san}$ cell preparation; most of these were Vα2^{lo} compared with 0.1% KLRG1^{hi} cells in the *Roquin*$^{+/+}$ cells (data not shown). It should be noted that SLEC-like cells were significantly reduced in *sanroque* OT-I mice compared with non–TCR-transgenic mice (data not shown).

By day 10 after transfer, all five mice that had received *Roquin*$^{san/san}$ OT-I cells developed diabetes, with near complete islet cell destruction (Fig. 3A, 3B). In contrast, none of the RIP-mOVA mice receiving *Roquin*$^{+/+}$ OT-I cells developed diabetes, and all had intact islets with little or no lymphocytic infiltrate (Fig. 3A, 3B). To exclude the possibility that the small difference in the starting population is an important contributor to the development of diabetes, we next sorted naive CD44^{lo} *Roquin*$^{san/san}$ OT-I or *Roquin*$^{+/+}$ OT-I cells and transferred them into RIP-mOVA mice. Adoptive transfer of 2×10^6 sorted naive (CD44^{lo}) OT-I cells from either *Roquin*$^{san/san}$ or *Roquin*$^{+/+}$ mice spiked with fixed numbers of B cells into nonirradiated RIP-mOVA recipients also caused autoimmune diabetes in RIP-mOVA mice receiving *Roquin*$^{san/san}$ CD44^{lo} OT-I 9 d later. None of the RIP-mOVA mice receiving *Roquin*$^{+/+}$ OT-I cells developed diabetes except for one, which had significantly lower blood glucose than the levels seen in recipients of *Roquin*$^{san/san}$ cells (data not shown).

To assess whether mice developing diabetes have increased numbers of SLECs, mice that became diabetic were sacrificed on day 10, and both total OT-I and OT-I SLECs were enumerated. Total numbers of OT-I cells were comparable in pancreatic lymph nodes, but there was a 10-fold increase in OT-I SLECs from *Roquin*$^{san/san}$ donors compared with recipients of *Roquin*$^{+/+}$ OT-I cells (Fig. 3C). These results demonstrate that *Roquin*$^{san/san}$ CD8$^+$ T cells readily differentiate into SLEC-like T cells and mediate autoimmune diabetes.

Enhanced effector properties in Roquin$^{san/san}$ *SLEC-like CD8$^+$ T cells*

Next, we investigated the effector properties of *Roquin*$^{san/san}$ SLEC-like CD8$^+$ T cells. IFN-γ and granzyme B are two important effector proteins for CD8$^+$ T cell-mediated killing. Intracellular flow cytometric staining revealed an ~6-fold increase in the proportion of IFN-γ–producing CD8$^+$ T cells, as well as a 2-fold increase in IFN-γ expression on a per-cell basis among CD44^{hi} CD8$^+$ T cells in *Roquin*$^{san/san}$ mice compared with wild-type littermates (Fig. 4A). KLRG1^{hi} SLEC-like CD8$^+$ T cells from *Roquin*$^{san/san}$ mice also expressed ~2-fold higher amounts of granzyme B than did their wild-type counterparts (Fig. 4B).

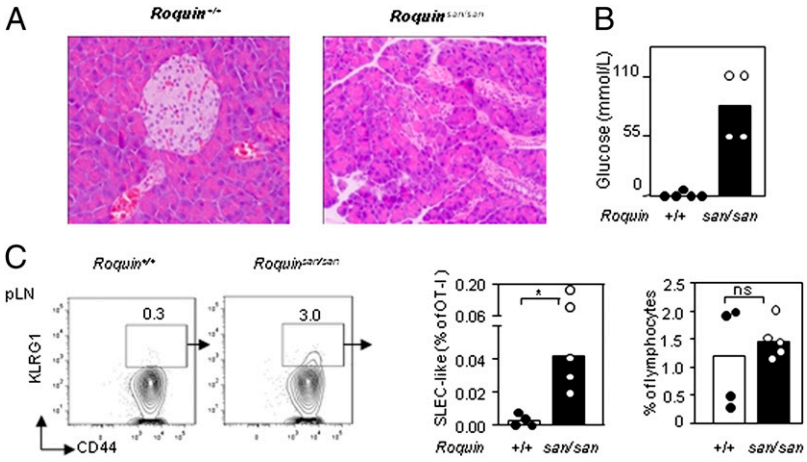

FIGURE 3. SLEC-like cells can trigger autoimmune diabetes in susceptible background. (**A**) Representative photomicrographs of H&E-stained pancreas sections from RIP-mOVA recipients of *Roquin*$^{+/+}$ (*left panel*) and *Roquin*$^{san/san}$ (*right panel*) OT-I cells. Original magnification ×40. (**B**) Urine glucose in RIP-mOVA recipients of MACS-purified *Roquin*$^{+/+}$ OT-I cells (open bar) and *Roquin*$^{san/san}$ OT-I cells (filled bar) 10 d after adoptive transfer. (**C**) *Left panels*, Representative flow cytometric contour plots showing KLRG1^{hi} SLEC-like cells gated on OT-I cells from pancreatic lymph node (pLN). Numbers represent the percentage of cells in the indicated gates. *Right panels*, Bar graphs showing the percentages of SLEC-like cells among total OT-I cells (*left panel*) and the percentages of OT-I cells among total lymphocytes (*right panel*). In (B) and (C), each symbol represents an individual mouse, and bars represent the median values for each group. All data are representative of two independent experiments. *$p < 0.05$.

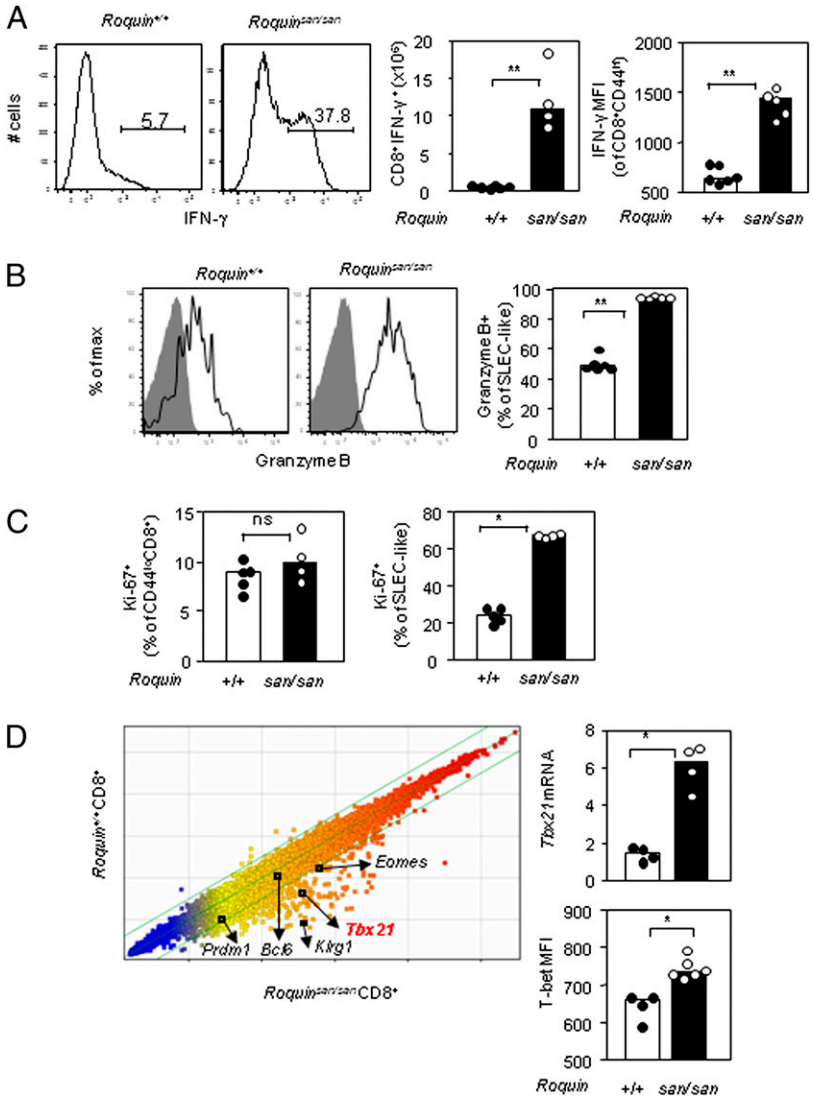

FIGURE 4. Enhanced effector properties in *Roquin*$^{san/san}$ SLEC-like CD8$^+$ T cells. (**A**) *Left panels*, Flow cytometric graphs showing the proportion of IFN-γ–producing splenic CD8$^+$ T cells. Numbers represent the percentage of cells in the indicated gates. *Right panels*, Bar graphs enumerating IFN-γ–producing splenic CD8$^+$ T cells (*left panel*) and showing IFN-γ MFI (*right panel*) among CD44^{hi}CD8$^+$ T cells from unimmunized *Roquin*$^{+/+}$ (open bar) and *Roquin*$^{san/san}$ (filled bars) mice. (**B**) Flow cytometric histograms showing granzyme B fluorescence intensity in SLEC-like cells from *Roquin*$^{+/+}$ (*left panel*) and *Roquin*$^{san/san}$ (*middle panel*) mice. Open histograms show the proportion of SLEC-like cells; shaded histograms show the proportion of CD44^{lo} CD8$^+$ T cells. Bar graph (*right panel*) showing granzyme B-producing cells among SLEC-like splenic CD8$^+$ T cells. (**C**) Bar graphs showing proportion of Ki-67$^+$ cells among CD44^{lo} CD8$^+$ T cells (*left panel*) and SLEC-like cells (*right panel*) in *Roquin*$^{+/+}$ (open bars) and *Roquin*$^{san/san}$ (filled bars) mice. (**D**) Microarray analysis of sorted naive CD8$^+$ T cells from *Roquin*$^{san/san}$ (n = 3) and *Roquin*$^{+/+}$ (n = 3) mice. Gene-expression values in naive *Roquin*$^{san/san}$ CD8$^+$ T cells versus naive *Roquin*$^{+/+}$ CD8$^+$ T cells analyzed with GeneChip Mouse Gene 1.0 ST Array (*left panel*). *Tbx21* mRNA normalized to *Gapdh* in sorted naive CD8$^+$ T cells from individual mouse spleens and pooled lymph nodes analyzed by real-time PCR (*top right panel*) and intracellular staining of T-bet protein in naive CD8$^+$ T cell (*bottom right panel*) from unimmunized *Roquin*$^{san/san}$ and *Roquin*$^{+/+}$ mouse spleens. Each symbol represents one mouse, and bars represent the median values for each group. All data are representative of two independent experiments. $*p < 0.05$, $**p < 0.005$.

To test whether accumulation of effector CD8$^+$ T cells in the presence of *Roquin*^{san} is a consequence of increased proliferation, cycling cells were enumerated by flow cytometry using Ki-67 staining. There was an ~3-fold increase in the proportion of cycling SLEC-like CD8$^+$ T cells in *Roquin*$^{san/san}$ mice compared with *Roquin*$^{+/+}$ littermates; the naive CD44^{lo} CD8$^+$ T cell compartment was unaffected (Fig. 4C).

Several transcription factors were shown to play critical roles in the differentiation and function of SLECs (10, 11, 13). To detect primary changes caused by the *san* mutation, we compared the gene-expression profiles of sorted naive *Roquin*$^{san/san}$ and *Roquin*$^{+/+}$ CD8$^+$ T cells. Naive cells were chosen to use in the comparative gene-expression profiling because KLRG1 was already upregulated in *Roquin*$^{san/san}$ naive CD8$^+$ T cells (Fig. 4D), and this approach had been successful in identifying *Icos* as one of the mRNAs responsible for Tfh cell accumulation within the CD4$^+$ compartment (33). *Klrg1* mRNA was increased by 20-fold in naive *Roquin*$^{san/san}$ CD8$^+$ T cells. Of the transcription factors known to influence effector/memory T cell differentiation—Eomesodermin (*Eomes*), Blimp (*Prdm1*), B cell lymphoma 6 (*Bcl6*), and T-bet (*Tbx21*)—*Tbx21*, a transcription factor required for terminal effector CD8$^+$ T cell differentiation, was significantly upregulated (Fig. 4D). This increase in T-bet within naive CD44^{lo} CD8$^+$ T cells was confirmed by real-time PCR and protein quantification by flow cytometry (Fig. 4D). Taken together, these data suggest that *Roquin*^{san} promotes the expression of IFN-γ, granzyme B, and T-bet responsible for increased SLEC formation and function.

T-bet reduction deviates the accumulation of activated CD8$^+$ T cells from SLEC-like cells to cells with a CD62L^{lo}KLRG1^{lo} phenotype

T-bet was shown to cooperate with Eomes to regulate SLEC and memory CD8$^+$ T cells (12, 36), and overexpression of T-bet can enhance SLEC formation in response to viral infection (12). Therefore, we hypothesized that the increased expression of T-bet observed above may cause the accumulation of self-reactive SLEC-like cells. We first investigated whether decreasing the gene dose of T-bet would have an impact on SLEC-like cell numbers. To do this, we crossed *sanroque* mice with *Duane* mice. Duane mice are homozygous for a missense point mutation in *Tbx21* (*Tbx21*$^{Du/Du}$) that causes a reduction in T-bet protein, and the residual protein found in these mice is defective (37). Decreasing the amount of T-bet did not decrease the accumulation of CD44^{hi} CD8$^+$ T cells in *Roquin*$^{san/san}$ *Tbx21*$^{Du/Du}$ mice that virtually lacked detectable T-bet protein (Fig. 5A, 5B). Nonetheless, SLEC-like cells were reduced by 4-fold in *Roquin*$^{san/san}$ *Tbx21*$^{Du/Du}$ mice compared with *Roquin*$^{san/san}$ *Tbx21*$^{+/+}$ mice, with *Roquin*$^{san/san}$ *Tbx21*$^{Du/+}$ mice

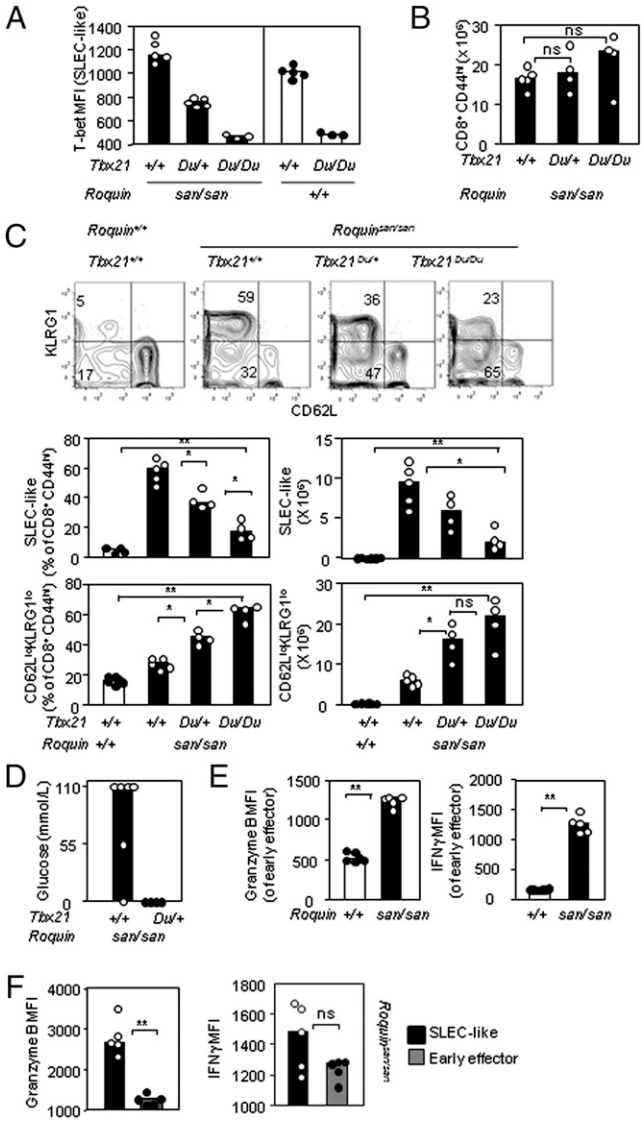

FIGURE 5. T-bet repression decreased the proportion of SLEC-like cells but not the total CD44^{hi} compartment. (**A**) Bar graph showing T-bet MFI in SLEC-like cells from spleens of unimmunized mice with the indicated genotypes. (**B**) Bar graph showing numbers of CD44^{hi} cells among splenic CD8$^+$ T cells in unimmunized *Roquin*$^{san/san}$ mice with decreasing *Tbx21* gene dosage. (**C**) Representative flow cytometric contour plots (*top panels*) showing the effect of reducing the gene dose of *Tbx21* on SLEC-like cells of spleens from unimmunized *Roquin*$^{+/+}$ and *Roquin*$^{san/san}$ mice. Numbers represent the percentage of cells in the indicated gates. Bar graphs (*bottom panels*) show the percentages and cell numbers of SLEC-like cells and CD62L^{lo}KLRG1^{lo} effectors among CD44^{hi} CD8$^+$ spleen cells from unimmunized *Roquin*$^{+/+}$ and *Roquin*$^{san/san}$ mice. (**D**) Urine glucose in RIP-mOVA recipients of MACS-purified *Roquin*$^{san/san}$ *Tbx21*$^{+/+}$ OT-I cells (○) and *Roquin*$^{san/san}$*Tbx21*$^{Du/+}$ OT-I cells (●) 8 d after adoptive transfer. Bar graphs showing MFI of granzyme B and IFN-γ of early effector (KLRG1^{lo}CD62L^{lo} CD44^{hi}) cells in *Roquin*$^{+/+}$ and *Roquin*$^{san/san}$ mice (**E**) and MFI of SLEC-like versus early effector CD8$^+$ T cells in *Roquin*$^{san/san}$ mice (**F**). Each symbol represents an individual mouse, and bars represent the median values in each group. Data are representative of five (A–C), one (D), or two (E, F) independent experiments. *$p < 0.05$, **$p < 0.005$, Mann–Whitney *U* test.

displaying an intermediate phenotype (Fig. 5C). The decrease in SLEC-like cells upon T-bet dose reduction was accompanied by an increase in CD62L^{lo}KLRG1^{lo} effector cells (Fig. 5C). Together, these data indicate that T-bet reduction deviates the accumulation of activated CD8$^+$ T cells from cells with a SLEC-like phenotype to CD62L^{lo}KLRG1^{lo} effector cells but is not responsible for the accumulation of effector CD8$^+$ T cells in *sanroque* mice.

T-bet reduction delays the onset of diabetes

We next examined whether reducing the expression of T-bet in *Roquin*$^{san/san}$ OT-I mice would decrease their diabetogenic potential. We transferred 2×10^6 OT-I cells from either *Roquin*$^{san/san}$ *Tbx21*$^{+/+}$ or *Roquin*$^{san/san}$*Tbx21*$^{Du/+}$ mice, spiked with fixed numbers of B cells, into nonirradiated RIP-mOVA recipients. On day 8, five of six mice receiving *Roquin*$^{san/san}$*Tbx21*$^{+/+}$ OT-I cells, but none of the recipients of *Roquin*$^{san/san}$*Tbx21*$^{Du/+}$ cells, were diabetic (Fig. 5D). Three of four recipients of *Roquin*$^{san/san}$ *Tbx21*$^{Du/+}$ OT-I cells and all recipients of *Roquin*$^{san/san}$ *Tbx21*$^{+/+}$ OT-I cells became diabetic 24 h later. Granzyme B and IFN-γ expression were still elevated in self-reactive *Roquin*$^{san/san}$ early effector cells, but their amounts were lower or comparable, respectively, to those of *Roquin*$^{san/san}$ SLEC-like cells (Fig. 5E, 5F). Together, these findings suggest that *Roquin*$^{san/san}$ SLEC-like cells play a key role in causing autoimmune diabetes in RIP-mOVA mice, and diabetes can be delayed by reducing T-bet expression.

Excessive IFN-γ signaling promotes the accumulation of Roquin$^{san/san}$ *SLEC-like CD8$^+$ T cells*

The fact that T-bet reduction could not reverse the accumulation of effector CD8$^+$ T cells in *Roquin*$^{san/san}$ mice prompted us to look into other causes. *Roquin*$^{san/san}$ CD4$^+$ T cells were shown to produce excessive amounts of two cytokines known to influence CD8$^+$ T cell homeostasis: IL-21 and IFN-γ (32). IL-21 is important for CD8$^+$ T cell survival and memory formation (38, 39), whereas IFN-γ promotes virus-specific CD8$^+$ T cell expansion (17, 40). Enumeration of SLEC-like cells in *Roquin*$^{san/san}$ mice deficient in IL-21 excluded dysregulation of this cytokine as the cause of SLEC-like cell accumulation in *Roquin*$^{san/san}$ mice (data not shown). Therefore, we investigated whether excessive IFN-γ production could explain the SLEC-phenotype and aberrant expansion of *Roquin*$^{san/san}$ effector CD8$^+$ T cells.

Roquin$^{san/san}$ mice were crossed with mice lacking the IFN-γ ligand-binding chain (also known as the α-chain) of the IFN-γR (*Ifngr1*$^{-/-}$). Loss of IFN-γ signaling almost completely reversed the accumulation of *Roquin*$^{san/san}$ SLEC-like cells (Fig. 6A) and reduced the absolute numbers of CD62L^{lo}KLRG1^{lo} CD8$^+$ T cells, with no appreciable effect on memory phenotype (CD62L^{hi}) cells, which remained comparable between *Roquin*$^{san/san}$ and *Roquin*$^{+/+}$ mice (data not shown). Lack of IFN-γ almost completely normalized the CD44^{hi} CD8$^+$ effector compartment in *Roquin*$^{san/san}$ mice: CD44^{hi} CD8$^+$ T cells in *Roquin*$^{san/san}$ *Ifngr1*$^{-/-}$ mice were only ~3-fold higher than in wild-type littermates (Fig. 6B) compared with the ~9-fold increase observed in *Roquin*$^{san/san}$ mice. The absolute number of SLEC-like cells and CD44^{hi} CD8$^+$ T cells in *Roquin*$^{+/+}$ *Ifng*$^{-/-}$ mice was comparable to those in their wild-type counterparts (Supplemental Fig. 1), suggesting that overproduction of IFN-γ, as seen in *Roquin*$^{san/san}$ mice, perturbs SLEC-like cell homeostasis. Together, these results suggest that IFN-γ is the predominant factor responsible for the expansion and accumulation of KLRG1^{hi} SLEC-like cells in *Roquin*$^{san/san}$ mice, but additional factors act to dysregulate this compartment (Fig. 6).

We also assessed the ability of *Roquin*$^{san/san}$ CD8$^+$ T cells deficient in IFN-γ production to induce autoimmune diabetes in susceptible RIP-mOVA mice by transferring 1 million sorted CD44^{lo} *Roquin*$^{san/san}$ *Ifng*$^{-/-}$ OT-I cells. Although none of the recipients became overtly diabetic, likely as a result of the smaller number of transferred cells, recipients of *Roquin*$^{san/san}$*Ifng*$^{-/-}$ OT-I cells preserved a larger number of islets/pancreas unit area compared with recipients of *Roquin*$^{san/san}$ OT-I cells (Supplemental Fig. 2). This result suggests

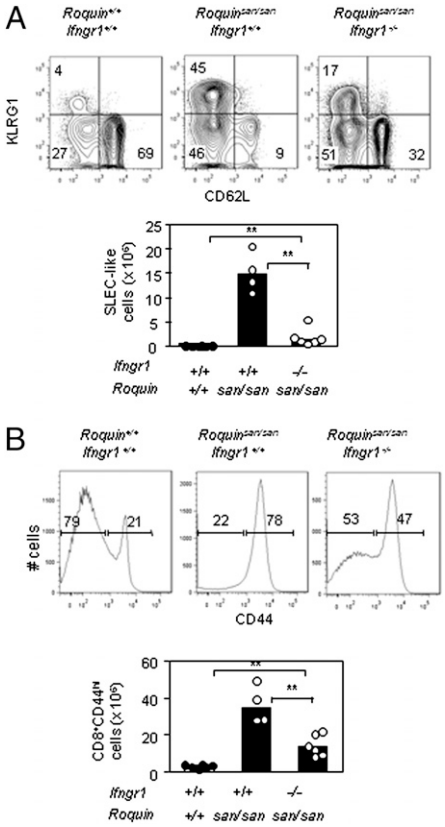

FIGURE 6. Loss of IFN-γ signaling prevents accumulation of *Roquin*$^{san/san}$ effector CD8$^+$ T cells. (**A**) Representative flow cytometric contour plots (*top panels*) showing the effect of losing IFN-γ signaling on the proportion of CD62L^{lo}KLRG1^{hi} (SLEC-like) cells among splenic CD8$^+$ CD44^{hi} T cells from 11-wk-old unimmunized *Roquin*$^{san/san}$ (*middle* and *right panels*) mice, deficient or not in IFN-γR1, compared with age-matched *Roquin*$^{+/+}$ (*left panel*) mice. Numbers represent the percentage of cells in the indicated gates. *Bottom panel*, Bar graph showing the numbers of CD62L^{lo}KLRG1^{hi} (SLEC-like) cells among CD8$^+$ CD44^{hi} T cells from unimmunized *Roquin*$^{+/+}$ (filled circles) and *Roquin*$^{san/san}$ (open circles) mice deficient or not in IFN-γR1. (**B**) Representative flow cytometric histograms (*top panels*) showing the effect of losing IFN-γ signaling on the proportion of CD44^{hi} cells among CD8$^+$ T cells from 11-wk-old unimmunized *Roquin*$^{san/san}$ (*middle* and *right panels*) mice, deficient or not in IFN-γR1, compared with age-matched *Roquin*$^{+/+}$ mice (*left panel*). Numbers represent the percentage of cells in the indicated gates. *Lower panel*, Bar graph showing the numbers of CD8$^+$CD44^{hi} T cells from unimmunized *Roquin*$^{+/+}$ (filled circles) and *Roquin*$^{san/san}$ (open circles) mice deficient or not in IFN-γR1. Each symbol represents an individual mouse, and bars represent the median values for each group. Data are representative of three independent experiments. $^{**}p < 0.005$.

that IFN-γ overproduction contributes to the increased ability of *Roquin*^{san} CD8$^+$ T cells to induce autoimmunity in a susceptible host.

Excessive IFN-γ promotes the overexpression of granzyme B and T-bet, as well as the proliferation of Roquin$^{san/san}$ *effector CD8$^+$ T cells*

Having observed that *Roquin*$^{san/san}$ CD8$^+$ effector T cells are more potent producers of granzyme B than are their wild-type counterparts (Fig. 4B), we sought to determine whether this might be a consequence of excessive IFN-γ production. Indeed, loss of IFN-γ signaling completely normalized granzyme B production by SLEC-like cells to wild-type levels (Fig. 7A).

IFN-γ is required to upregulate T-bet in CD8$^+$ T cells in an indirect manner upon virus infection (12, 41). We wondered whether the increased expression of T-bet in *Roquin*$^{san/san}$ mice is a consequence of excessive IFN-γ. To assess this, we measured T-bet mean fluorescence intensity (MFI) in naive (CD44^{lo}) CD8$^+$ T cells and SLEC-like cells from *Roquin*$^{san/san}$ mice deficient or not in IFN-γR1. In the absence of IFN-γR signaling, T-bet expression in *Roquin*$^{san/san}$ SLEC-like cells was comparable to that of *Roquin*$^{+/+}$ mice (Fig. 7B). A decrease in T-bet expression was also observed in the naive CD8$^+$ T cell compartment in *Roquin*$^{san/san}$*Ifngr1*$^{-/-}$ mice, although T-bet amounts were still higher than were those of *Roquin*$^{+/+}$ mice (Fig. 7C), suggesting that other factors contribute to elevated T-bet expression in naive CD8$^+$ T cells.

IFN-γ was shown to promote Ag-specific CD8$^+$ T cell expansion during viral infections (17, 40), and we showed that *Roquin*$^{san/san}$ CD8$^+$ T cells are hyperproliferative (Fig. 2C). To formally test whether excessive IFN-γ drives CD8$^+$ effector T cell accumulation through enhancing their proliferation, cycling (Ki-67$^+$) cells were enumerated. Proliferating CD8$^+$ T cells were reduced by half in the absence of IFN-γR1 (Fig. 7D). IFN-γR signaling acted on CD62L^{lo}KLRG1^{lo} effector CD8$^+$ T cells, whose proliferative rate was corrected with wild-type levels in mice lacking IFN-γR1, but it did not influence the proliferation of SLEC-like cells themselves (Fig. 7D).

Together, these data suggest that excessive IFN-γ predominantly acts by enhancing the cytotoxic potential and T-bet transcription of SLEC-like CD8$^+$ T cells, but it only affects the proliferative rate of CD62L^{lo}KLRG1^{lo} effector CD8$^+$ T cells.

Roquin^{san} *represses Ifng mRNA decay*

Our results showed that IFN-γ dysregulation explains SLEC-like cell accumulation driven by *Roquin*^{san}. To understand the mechanism by which *Roquin*^{san} causes IFN-γ overproduction by CD8$^+$ T cells, we asked whether, as described for *Icos* (33), this accumulation occurred at the level of *Ifng* mRNA. Purified *Roquin*$^{san/san}$ and *Roquin*$^{+/+}$ CD44^{lo} CD8$^+$ T cells were subjected to in vitro activation in the presence of anti-CD3, anti-CD28, and IL-12 for 16 h. *Ifng* mRNA was ~60-fold higher in activated *Roquin*$^{san/san}$ CD8$^+$ T cells compared with wild-type counterparts (Fig. 8A). Given the reported enhancement of *Icos* mRNA stability by *Roquin*^{san} (30, 33), we tested whether IFN-γ overproduction was due to the prolonged half-life of *Ifng* mRNA. Naive CD44^{lo} CD8$^+$ T cells of *Roquin*$^{san/san}$ and *Roquin*$^{+/+}$ mice were treated with actinomycin D 16 h after activation to inhibit mRNA transcription. *Ifng* mRNA was measured at different intervals after treatment. *Roquin*^{san} prolonged the half-life of *Ifng* mRNA by >18-fold (Fig. 8B). Thus, overproduction of IFN-γ by *Roquin*$^{san/san}$ CD8$^+$ T cells is a consequence of failed posttranscriptional repression of *Ifng* expression.

Discussion

The nature and regulation of KLRG1^{hi} CD8$^+$ T cells that develop in the absence of immunization have been obscure. The data in this study reveal that these SLEC-like cells accumulate in mice prone to autoimmunity, in particular *Roquin*$^{san/san}$ mice, which were shown previously to develop lupus and to be more susceptible to autoimmune diabetes. Our work reveals that overproduction of IFN-γ is, in large part, responsible for the pathogenic accumulation of SLEC-like CD8$^+$ T cells.

A very recent report demonstrated that Roquin deletion in T cells caused an ~6.5-fold increase in CD62L^{lo}CD44^{hi} effector-like CD8$^+$ T cells, an increase in KLRG1^{hi} CD8$^+$ T cells, and a decrease in naive and memory-like CD8$^+$ T cells (28). In contrast, *Roquin*$^{san/san}$ mice bearing a point mutation (Met^{199} to Arg substitution) in the RNA-binding ROQ domain in Roquin display an increase in effector-like CD8$^+$ T cells (SLEC-like cells and

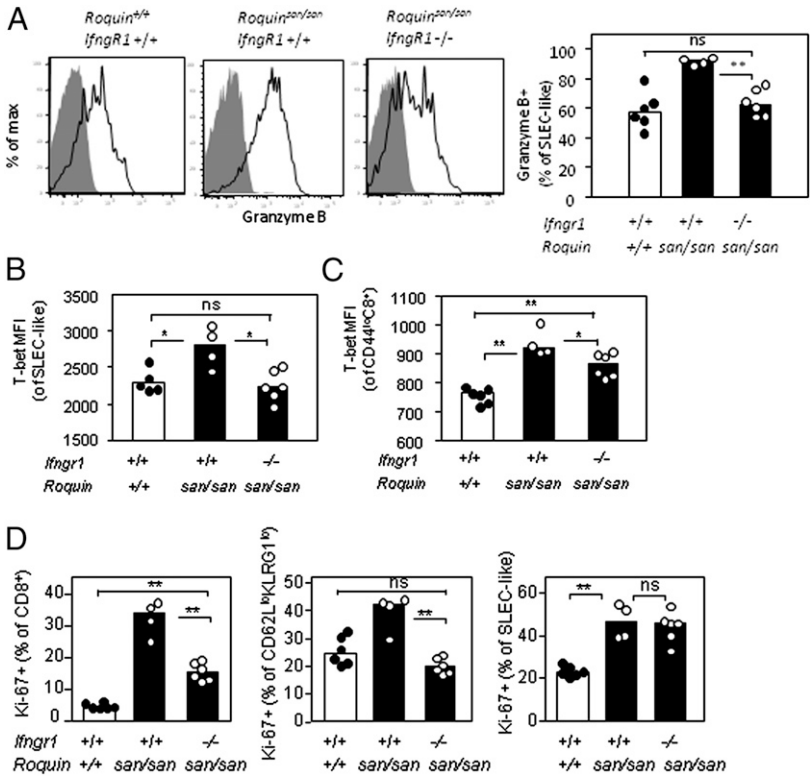

FIGURE 7. Loss of IFN-γ signaling alleviates the overexpressing effector phenotypes of *Roquin*$^{san/san}$ SLEC-like cells. (**A**) Flow cytometric histograms (three *left panels*) showing granzyme B fluorescence intensity in SLEC-like cells from *Roquin*$^{+/+}$ (*left panel*) and *Roquin*$^{san/san}$ (*middle* and *right panels*) mice, deficient or not in IFN-γR1. Open histograms show the proportion of SLEC-like cells; shaded histograms show the proportion of CD44^{lo} CD8^{+} T cells. *Right panel*, Bar graph showing granzyme B-producing cells among SLEC-like splenic CD8^{+} T cells. Bar graphs showing T-bet MFI in SLEC-like cells (**B**) and naive CD44^{lo} CD8^{+} T cells (**C**) from unimmunized *Roquin*$^{+/+}$ (open bars), and *Roquin*$^{san/san}$ (filled bars) mice, deficient or not in IFN-γR1. (**D**) Bar graphs showing the proportion of Ki-67^{+} cells among total CD8^{+} (*left panel*), CD62L^{lo} KLRG1^{lo} (*middle panel*), and SLEC-like (*right panel*) cells from unimmunized *Roquin*$^{+/+}$ (open bars) and *Roquin*$^{san/san}$ (filled bars) mice, deficient or not in IFN-γR1. Each symbol represents an individual mouse, and bars represent the median values for each group. Data are representative of two independent experiments. $*p < 0.05$, $**p < 0.005$.

CD62L^{lo}KLRG1^{lo} CD44^{hi} CD8^{+} T cells) but no changes in the absolute number of naive CD8^{+} and resting memory-like CD8^{+} T cells. Unlike *Roquin*$^{san/san}$ mice, *Roquin*-null mice do not develop autoimmunity. These contrasting phenotypes can be partially explained by intact RING-mediated activity in *Roquin*$^{san/san}$ mice, which opposes the action of the RNA-binding ROQ and CCCH domains through a different mechanism (R. Ramiscal and C.G. Vinuesa, unpublished observations). Thus, it is likely that Roquin controls CD8^{+} T cell homeostasis through several mechanisms. This work allows dissection of the contribution of Roquin-mediated RNA regulation to this effect.

Our work highlights the crucial role for posttranscriptional repression of *Ifng* mRNA in the control of naturally occurring CD8^{+} T cell effector cells, including those harboring self-reactivities. Failure to repress *Ifng* mRNA caused by the *san* mutation in *Roquin* is a major contributor to the aberrant accumulation of SLEC-like CD8^{+} T cell effectors. Posttranscriptional repression of IFN-γ emerges as a powerful mechanism to control the expansion of highly cytotoxic SLEC-like cells.

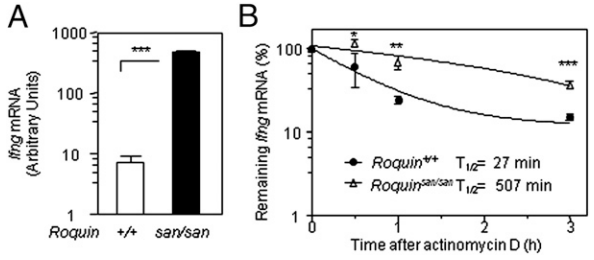

FIGURE 8. Excessive IFN-γ drives the SLEC-like cell accumulation in *Roquin*$^{san/san}$ mice. (**A**) *Ifng* mRNA normalized to *Hprt* in sorted CD44^{lo} CD8^{+} T cells activated in vitro for 16 h from mouse spleens and pooled lymph nodes analyzed by real-time PCR ($n = 3$). (**B**) *Ifng* mRNA in sorted *Roquin*$^{san/san}$ and *Roquin*$^{+/+}$ CD44^{lo} CD8^{+} T cells activated in vitro for 16 h and treated with actinomycin D for the times indicated. Endogenous *Ifng* mRNA levels were measured using real-time RT-PCR and normalized to *Hprt*. The amount of *Ifng* mRNA at time 0 h was assigned 100%. Data are shown as mean ± SD ($n = 3$). Data were analyzed with GraphPad Prism using the nonlinear regression-one phase decay equation. Bars represent the mean values for each group (A), and each symbol represents the mean value from three mice (B). Data are representative of two independent experiments. $*p < 0.05$, $**p < 0.005$, $***p < 0.0005$, unpaired t test.

A role for IFN-γ as the principal effector cytokine of CD8^{+} T cell-mediated immunity has long since been established (42). In the last decade, dual opposing roles for IFN-γ in the homeostatic control of T cells were also described (17, 25, 40): IFN-γ limits the expansion of T cells through stimulating the expression of caspases downstream of Fas (25), and, paradoxically, it can also enhance expansion of CD8^{+} T cell effector clones during viral infection (17) through an unknown molecular mechanism. Our study establishes a new role for IFN-γ in the control of naturally occurring CD8^{+} T cell effectors and highlights the importance of controlled posttranscriptional regulation of this cytokine: IFN-γ overproduction in the presence of *Roquin*^{san} promotes the proliferation of KLRG1^{lo} effectors and the formation of highly cytotoxic SLEC-like cells and increases MHC-I expression on APCs, which promotes CD8^{+} T cell activation (Supplemental Fig. 3).

Roquin was reported to bind to and repress *Icos* mRNA (29, 30, 33); prolonged *Icos* mRNA stability in the presence of *Roquin*^{san} contributes to aberrant accumulation of CD4^{+} Tfh cells and lupus. The present work identifies IFN-γ as a novel target of *Roquin*^{san}-mediated repression. IFN-γ is a cytokine known to be regulated posttranscriptionally: the RNA-binding protein tristetraprolin was reported to destabilize IFN-γ mRNA (43). Accumulation of *Ifng* mRNA causes excessive production of IFN-γ, which acts, at least in part, to promote the expansion and accumulation of KLRG1^{lo} and terminally differentiated effector CD8^{+} T cells in *Roquin*$^{san/san}$ mice.

In summary, we described a novel posttranscriptional mechanism operating to regulate SLEC-like cell homeostasis and prevent the accumulation of self-reactive CD8^{+} effectors, as well as their cytotoxic potential. Aberrant accumulation of highly cytotoxic

SLEC-like cells, despite their short lifespan, can pose a threat for autoimmunity. Thus, manipulation of this axis to curtail the expansion and survival of self-reactive SLECs may be useful to dampen the pathological accumulation of these cells that is often seen in inflammatory diseases and that was shown in this study to contribute to autoimmune diabetes.

Acknowledgments

We thank Axel Kallies (Walter and Eliza Hall Institute of Medical Research) for critical reading of the manuscript, Kaiman Peng and Stephen Ohm (Australian Cancer Research Foundation Biomolecular Resource Facility, JCSMR) for help with microarray gene profiling and analysis, Anne Prins (Microscopy and Cytometry Resource Facility, JCSMR) for H&E stains, Harpreet Vohra and Michael Devoy (Microscopy and Cytometry Resource Facility, JCSMR) for assistance with cell sorting, and Michael Devoy for processing H&E-stained pancreas section images prior to islet quantification.

Disclosures

The authors have no financial conflicts of interest.

References

1. Babbe, H., A. Roers, A. Waisman, H. Lassmann, N. Goebels, R. Hohlfeld, M. Friese, R. Schröder, M. Deckert, S. Schmidt, et al. 2000. Clonal expansions of CD8(+) T cells dominate the T cell infiltrate in active multiple sclerosis lesions as shown by micromanipulation and single cell polymerase chain reaction. *J. Exp. Med.* 192: 393–404.
2. Friese, M. A., and L. Fugger. 2009. Pathogenic CD8(+) T cells in multiple sclerosis. *Ann. Neurol.* 66: 132–141.
3. Qin, H., J. D. Trudeau, G. S. Reid, I. F. Lee, J. P. Dutz, P. Santamaria, C. B. Verchere, and R. Tan. 2004. Progression of spontaneous autoimmune diabetes is associated with a switch in the killing mechanism used by autoreactive CTL. *Int. Immunol.* 16: 1657–1662.
4. Tsai, S., A. Shameli, and P. Santamaria. 2008. CD8+ T cells in type 1 diabetes. *Adv. Immunol.* 100: 79–124.
5. Bhatnagar, A., J. D. Wig, and S. Majumdar. 2001. Expression of activation, adhesion molecules and intracellular cytokines in acute pancreatitis. *Immunol. Lett.* 77: 133–141.
6. Bisping, G., N. Lügering, S. Lütke-Brintrup, H. G. Pauels, G. Schürmann, W. Domschke, and T. Kucharzik. 2001. Patients with inflammatory bowel disease (IBD) reveal increased induction capacity of intracellular interferon-gamma (IFN-gamma) in peripheral CD8+ lymphocytes co-cultured with intestinal epithelial cells. *Clin. Exp. Immunol.* 123: 15–22.
7. Blanco, P., V. Pitard, J. F. Viallard, J. L. Taupin, J. L. Pellegrin, and J. F. Moreau. 2005. Increase in activated CD8+ T lymphocytes expressing perforin and granzyme B correlates with disease activity in patients with systemic lupus erythematosus. *Arthritis Rheum.* 52: 201–211.
8. Suzuki, T., M. Ito, N. Hayasaki, A. Ishihara, T. Ando, K. Ina, and K. Kusugami. 2003. Cytotoxic molecules expressed by intraepithelial lymphocytes may be involved in the pathogenesis of acute gastric mucosal lesions. *J. Gastroenterol.* 38: 216–221.
9. Intlekofer, A. M., A. Banerjee, N. Takemoto, S. M. Gordon, C. S. Dejong, H. Shin, C. A. Hunter, E. J. Wherry, T. Lindsten, and S. L. Reiner. 2008. Anomalous type 17 response to viral infection by CD8+ T cells lacking T-bet and eomesodermin. *Science* 321: 408–411.
10. Intlekofer, A. M., N. Takemoto, C. Kao, A. Banerjee, F. Schambach, J. K. Northrop, H. Shen, E. J. Wherry, and S. L. Reiner. 2007. Requirement for T-bet in the aberrant differentiation of unhelped memory CD8+ T cells. *J. Exp. Med.* 204: 2015–2021.
11. Pearce, E. L., A. C. Mullen, G. A. Martins, C. M. Krawczyk, A. S. Hutchins, V. P. Zediak, M. Banica, C. B. DiCioccio, D. A. Gross, C. A. Mao, et al. 2003. Control of effector CD8+ T cell function by the transcription factor Eomesodermin. *Science* 302: 1041–1043.
12. Joshi, N. S., W. Cui, A. Chandele, H. K. Lee, D. R. Urso, J. Hagman, L. Gapin, and S. M. Kaech. 2007. Inflammation directs memory precursor and short-lived effector CD8(+) T cell fates via the graded expression of T-bet transcription factor. *Immunity* 27: 281–295.
13. Kallies, A., A. Xin, G. T. Belz, and S. L. Nutt. 2009. Blimp-1 transcription factor is required for the differentiation of effector CD8(+) T cells and memory responses. *Immunity* 31: 283–295.
14. Rutishauser, R. L., G. A. Martins, S. Kalachikov, A. Chandele, I. A. Parish, E. Meffre, J. Jacob, K. Calame, and S. M. Kaech. 2009. Transcriptional repressor Blimp-1 promotes CD8(+) T cell terminal differentiation and represses the acquisition of central memory T cell properties. *Immunity* 31: 296–308.
15. Rao, R. R., Q. Li, K. Odunsi, and P. A. Shrikant. 2010. The mTOR kinase determines effector versus memory CD8+ T cell fate by regulating the expression of transcription factors T-bet and Eomesodermin. *Immunity* 32: 67–78.
16. Tripathi, P., S. Kurtulus, S. Wojciechowski, A. Sholl, K. Hoebe, S. C. Morris, F. D. Finkelman, H. L. Grimes, and D. A. Hildeman. 2010. STAT5 is critical to maintain effector CD8+ T cell responses. *J. Immunol.* 185: 2116–2124.
17. Whitmire, J. K., J. T. Tan, and J. L. Whitton. 2005. Interferon-gamma acts directly on CD8+ T cells to increase their abundance during virus infection. *J. Exp. Med.* 201: 1053–1059.
18. Srinivasan, M., and K. A. Frauwirth. 2009. Peripheral tolerance in CD8+ T cells. *Cytokine* 46: 147–159.
19. Chen, G., A. K. Tai, M. Lin, F. Chang, C. Terhorst, and B. T. Huber. 2007. Increased proliferation of CD8+ T cells in SAP-deficient mice is associated with impaired activation-induced cell death. *Eur. J. Immunol.* 37: 663–674.
20. Davey, G. M., C. Kurts, J. F. Miller, P. Bouillet, A. Strasser, A. G. Brooks, F. R. Carbone, and W. R. Heath. 2002. Peripheral deletion of autoreactive CD8 T cells by cross presentation of self-antigen occurs by a Bcl-2-inhibitable pathway mediated by Bim. *J. Exp. Med.* 196: 947–955.
21. Twu, Y. C., M. R. Gold, and H. S. Teh. 2011. TNFR1 delivers pro-survival signals that are required for limiting TNFR2-dependent activation-induced cell death (AICD) in CD8+ T cells. *Eur. J. Immunol.* 41: 335–344.
22. Goodnow, C. C., J. Sprent, B. Fazekas de St Groth, and C. G. Vinuesa. 2005. Cellular and genetic mechanisms of self tolerance and autoimmunity. *Nature* 435: 590–597.
23. Saikali, P., J. P. Antel, C. L. Pittet, J. Newcombe, and N. Arbour. 2010. Contribution of astrocyte-derived IL-15 to CD8 T cell effector functions in multiple sclerosis. *J. Immunol.* 185: 5693–5703.
24. Shevach, E. M., R. A. DiPaolo, J. Andersson, D. M. Zhao, G. L. Stephens, and A. M. Thornton. 2006. The lifestyle of naturally occurring CD4+ CD25+ Foxp3+ regulatory T cells. *Immunol. Rev.* 212: 60–73.
25. Refaeli, Y., L. Van Parijs, S. I. Alexander, and A. K. Abbas. 2002. Interferon gamma is required for activation-induced death of T lymphocytes. *J. Exp. Med.* 196: 999–1005.
26. Voehringer, D., C. Blaser, P. Brawand, D. H. Raulet, T. Hanke, and H. Pircher. 2001. Viral infections induce abundant numbers of senescent CD8 T cells. *J. Immunol.* 167: 4838–4843.
27. Boyman, O., J. H. Cho, J. T. Tan, C. D. Surh, and J. Sprent. 2006. A major histocompatibility complex class I-dependent subset of memory phenotype CD8+ cells. *J. Exp. Med.* 203: 1817–1825.
28. Bertossi, A., M. Aichinger, P. Sansonetti, M. Lech, F. Neff, M. Pal, F. T. Wunderlich, H. J. Anders, L. Klein, and M. Schmidt-Supprian. 2011. Loss of Roquin induces early death and immune deregulation but not autoimmunity. *J. Exp. Med.* 208: 1749–1756.
29. Athanasopoulos, V., A. Barker, D. Yu, A. H. Tan, M. Srivastava, N. Contreras, J. Wang, K. P. Lam, S. H. Brown, C. C. Goodnow, et al. 2010. The ROQUIN family of proteins localizes to stress granules via the ROQ domain and binds target mRNAs. *FEBS J.* 277: 2109–2127.
30. Glasmacher, E., K. P. Hoefig, K. U. Vogel, N. Rath, L. Du, C. Wolf, E. Kremmer, X. Wang, and V. Heissmeyer. 2010. Roquin binds inducible costimulator mRNA and effectors of mRNA decay to induce microRNA-independent post-transcriptional repression. *Nat. Immunol.* 11: 725–733.
31. Linterman, M. A., R. J. Rigby, R. K. Wong, D. Yu, R. Brink, J. L. Cannons, P. L. Schwartzberg, M. C. Cook, G. D. Walters, and C. G. Vinuesa. 2009. Follicular helper T cells are required for systemic autoimmunity. *J. Exp. Med.* 206: 561–576.
32. Vinuesa, C. G., M. C. Cook, C. Angelucci, V. Athanasopoulos, L. Rui, K. M. Hill, D. Yu, H. Domaschenz, B. Whittle, T. Lambe, et al. 2005. A RING-type ubiquitin ligase family member required to repress follicular helper T cells and autoimmunity. *Nature* 435: 452–458.
33. Yu, D., A. H. Tan, X. Hu, V. Athanasopoulos, N. Simpson, D. G. Silva, A. Hutloff, K. M. Giles, P. J. Leedman, K. P. Lam, et al. 2007. Roquin represses autoimmunity by limiting inducible T-cell co-stimulator messenger RNA. *Nature* 450: 299–303.
34. Izui, S., R. Merino, L. Fossati, and M. Iwamoto. 1994. The role of the Yaa gene in lupus syndrome. *Int. Rev. Immunol.* 11: 211–230.
35. Kurts, C., H. Kosaka, F. R. Carbone, J. F. Miller, and W. R. Heath. 1997. Class I-restricted cross-presentation of exogenous self-antigens leads to deletion of autoreactive CD8(+) T cells. *J. Exp. Med.* 186: 239–245.
36. Intlekofer, A. M., N. Takemoto, E. J. Wherry, S. A. Longworth, J. T. Northrup, V. R. Palanivel, A. C. Mullen, C. R. Gasink, S. M. Kaech, J. D. Miller, et al. 2005. Effector and memory CD8$^+$ T cell fate coupled by T-bet and eomesodermin. *Nat. Immunol.* 6: 1236–1244.
37. Jenne, C. N., A. Enders, R. Rivera, S. R. Watson, A. J. Bankovich, J. P. Pereira, Y. Xu, C. M. Roots, J. N. Beilke, A. Banerjee, et al. 2009. T-bet-dependent S1P5 expression in NK cells promotes egress from lymph nodes and bone marrow. *J. Exp. Med.* 206: 2469–2481.
38. Novy, P., X. Huang, W. J. Leonard, and Y. Yang. 2011. Intrinsic IL-21 signaling is critical for CD8 T cell survival and memory formation in response to vaccinia viral infection. *J Immunol.* 186: 2729–2738.
39. Yi, J. S., J. T. Ingram, and A. J. Zajac. 2010. IL-21 deficiency influences CD8 T cell quality and recall responses following an acute viral infection. *J. Immunol.* 185: 4835–4845.
40. Badovinac, V. P., A. R. Tvinnereim, and J. T. Harty. 2000. Regulation of antigen-specific CD8+ T cell homeostasis by perforin and interferon-gamma. *Science* 290: 1354–1358.
41. Cui, W., N. S. Joshi, A. Jiang, and S. M. Kaech. 2009. Effects of Signal 3 during CD8 T cell priming: Bystander production of IL-12 enhances effector T cell expansion but promotes terminal differentiation. *Vaccine* 27: 2177–2187.
42. Billiau, A., and P. Matthys. 2009. Interferon-gamma: a historical perspective. *Cytokine Growth Factor Rev.* 20: 97–113.
43. Ogilvie, R. L., J. R. Sternjohn, B. Rattenbacher, I. A. Vlasova, D. A. Williams, H. H. Hau, P. J. Blackshear, and P. R. Bohjanen. 2009. Tristetraprolin mediates interferon-gamma mRNA decay. *J. Biol. Chem.* 284: 11216–11223.

Breakdown in Repression of IFN-γ mRNA Leads to Accumulation of Self-Reactive Effector CD8$^+$ T Cells

Pheh-Ping Chang, Sau K. Lee, Xin Hu, Gayle Davey, Guowen Duan, Jae-Ho Cho, Guna Karupiah, Jonathan Sprent, William R. Heath, Edward M. Bertram and Carola G. Vinuesa

J Immunol 2012; 189:701-710; Prepublished online 8 June 2012;
doi: 10.4049/jimmunol.1102432
http://www.jimmunol.org/content/189/2/701

The Journal of Immunology is published twice each month by
The American Association of Immunologists, Inc.,
9650 Rockville Pike, Bethesda, MD 20814-3994.

Print ISSN: 0022-1767 Online ISSN: 1550-6606.